Direct re-lithiation strategy for spent lithium iron phosphate battery in Li-based eutectic using organic reducing agents

Tanongsak Yingnakorn,[1] Jennifer Hartley,[1] Jason S. Terreblanche,[1] Chunhong Lei,[1] Wesley Dose,[1,2] Andrew P Abbott*[1]

[1] *School of Chemistry, University of Leicester, Leicester, LE1 7RH, United Kingdom*

[2] *School of Chemistry, University of New South Wales, Sydney NSW 2052 Australia*

**apa1@le.ac.uk*

Supplementary Information

Table S1 Starting materials and processes for the synthesis of $LiFePO_4$.

Li Source	P Source	Fe Source	Calcination Conditions	Contributor
Li_2CO_3	$(NH_4)_2HPO_4$	$Fe_3(PO_4)_2.8H_2O$	800ºC for 48 hr in N_2	MIT (1967) [1]
Li_2CO_3	$(NH_4)_2HPO_4$	$Fe(CH_3CO_2)_2$	800ºC for 24 hr in Ar	Goodenough (1997) [2]
Li_2CO_3	$(NH_4)_2HPO_4$	$FeC_2O_4.2H_2O$	800ºC for 36 hr in N_2	Sweden (2000) [3]
Li_3PO_4	$Fe_3(PO_4)_2.8H_2O$		700ºC for 7 hr in Ar	Sweden (2003) [3]
$LiNO_3$	$(NH_4)_2HPO_4$	$Fe_3(NO_3)_3.9H_2O$	750ºC for 12 hr in Ar	Komaba (2004) [3]
LiCl	H_3PO_4	$FeCl_2.4H_2O$	700ºC for 12 hr in N_2	Nazar (2001) [3]
Li_2CO_3	$NH_4H_2PO_4$	$Fe(CH_3CO_2)_2$	550ºC for 24 hr in N_2	Sony (2001) [4]
Li_2CO_3	$Fe[(C_6H_5PO_3.H_2O)]$		>600ºC for >16 hr in N_2	Italy (2004) [3]
Li_2CO_3	$NH_4H_2PO_4$	$FeC_2O_4.2H_2O$	600ºC - 800ºC in Ar	MIT and A123 Systems (2002) [5]
LiH_2PO_4		Fe_2O_3	750ºC for 8 hr	Valance (2003) [3]

			in Ar	
$Li_3PO_4 \cdot 0.5H_2O$	$FePO_4$	$FePO_4$, Fe	600ºC for 30 min. in Ar	SJTU and Ma (2004) [6]

Disassembly and confirmation of the active material and binder

The spent lithium iron phosphate battery was dismantled, and the electrodes were washed in dimethyl carbonate (DMC) for 24 hours. The dismantled materials consist of $LiFePO_4$-on-aluminium cathodes, graphite-on-copper anodes, and a pouch case. The cathode electrode was used as the raw material for this experiment. The total average thickness of the intact cathode is 199.20 (±2.43) µm, as determined via SEM imaging of the electrode cross-section, as shown in **Figure S1a**. This consists of three layers, an aluminium foil current collector (29.59 (±1.65) µm thick) sandwiched between two layers of active cathode material (80.85 (±1.25) µm and 88.76 (±2.47) µm). At the electrode surface, the particle sizes are inhomogeneous, with a dimension range of about 200 nm to 1 µm (**Figure S1b**). EDX analysis confirmed the Fe:P:O atomic ratio in the cathode active material to be 1: 1.02(0.02): 4.04(0.11) (see the **Table S2**), as would be expected for either $FePO_4$ or $LiFePO_4$. The X-ray diffraction peaks of the initially spent $LiFePO_4$ cathode plate, water-delaminated, and ground cathode powder are shown in **Figure S2**, and compared to standard $LiFePO_4$ (COD 4001848) and standard $FePO_4$ (COD 1525576). All three samples were confirmed to be the $LiFePO_4$ olivine structure, but were observed to also contain a small amount of $FePO_4$.

a) b)

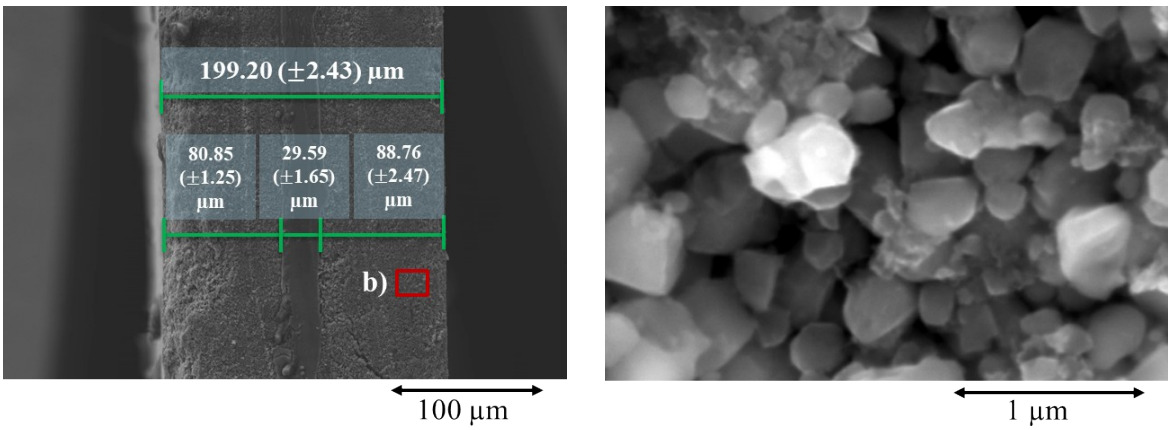

c)

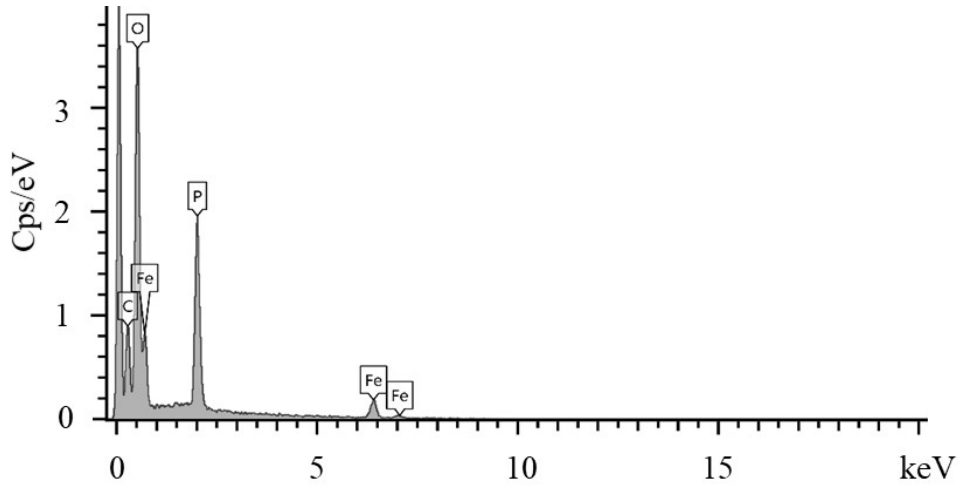

Figure S1: SEM image of a) the $LiFePO_4$ cathode cross-session, b), and c) image and the EDX spectrum of the cathode area (highlight red areas).

Table S2 EDX elemental composition of initial cathode (Figure S1b)

Element	Wt%	Atomic%	Atomic ratio
C	18.23(3.94)	31.64(5.95)	2.83(0.60)
O	34.77(2.09)	45.59(4.24)	4.04(0.11)
P	16.96(0.88)	11.48(0.97)	1.02(0.02)
Fe	30.05(0.98)	11.28(0.74)	1.00(0.00)

Atomic ratio is calculated refer to Fe

Thermal analysis curves were measured for the spent $LiFePO_4$ cathode and were compared with reference materials prepared from uncycled $LiFePO_4$ with either CMC/SBR or with PVDF (90:5:5 weight ratio of $LiFePO_4$, carbon black, and binder, respectively). These binders were selected as they are the most common commercially used binders [7-9], and it can be detected by weight loss, while $LiFePO_4$ itself will not show significant mass change below the temperature of 430 °C [10]. It can be seen from **Figure S2a** that the most likely binder in the $LiFePO_4$ cathode sample is CMC/SBR, even though there is a difference in the weight loss. This may be due to a difference in weight ratio of binder-to-active material in the two samples, as CMC/SBR is water-miscible and has a high probability of being leached from the active material during the water delamination step.

This identification is confirmed via the TGA and DTG results in **Figure S2b**, where it can be seen that there are three main mass loss processes. The first takes place from 25-180 °C (ca. 0.69 % mass loss), which probably results from the evaporation of moisture in the cathode. The second takes place from ca. 180-330 °C (ca. 1.5%), and the third takes place at 330-490 °C (ca. 1.15% mass loss). The DSC curve indicates a change in heat flow consumed in the sample within the first region (25-180 °C), agreeing with the suggestion of moisture evaporation, but does not have noticeable peaks of heat flow release for the other mass loss processes indicated by TGA. Additionally, at a temperature range of 460-480 °C, there is an exothermic peak that is not immediately identifiable as belonging to a mass loss process but it might relate with the thermal decomposition of the carbonaceous coating and carbon remaining from mixing slurry [11, 12].

Figure S2c and **S2d** are the TGA and DTG curves comparing spent $LiFePO_4$ cathode, CMC-SBR mixture, pure CMC, and PVDF binders. It is clear that the CMC curve shows two central changing regions (ca. 25-180 °C and 180-330 °C) of weight loss, the CMC-SBR shows three central changing regions (ca. 25-180 °C, 180-330 °C, and 330-490 °C), while PVDF shows only one significant changing region (ca. 350-500 °C). Therefore, it can be concluded that the CMC-SBR is correspondingly matched with the binder used in the spent $LiFePO_4$ cathode in this current study. The presence of CMC/SBR is beneficial due to its water-miscibility, as all the active material could be in contact with the oxidising and re-lithiation solvents. If PVDF was present, it could potentially result in active material not reacting due to being encapsulated.

a)

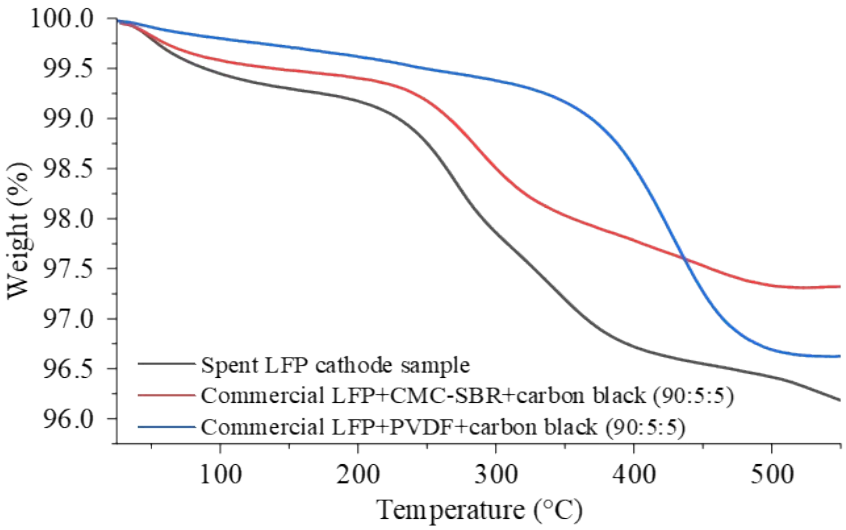
100.0
99.5
99.0
98.5
98.0
97.5
97.0
96.5
96.0
Weight (%)
100
200
300
400
500
Temperature (°C)
Spent LFP cathode sample
Commercial LFP+CMC-SBR+carbon black (90:5:5)
Commercial LFP+PVDF+carbon black (90:5:5)

b)

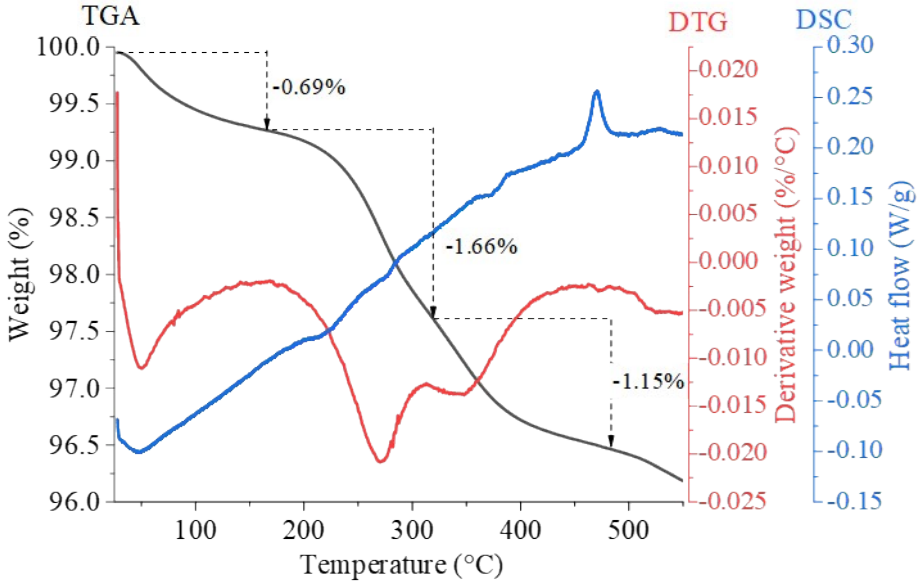
TGA
DTG
DSC
100.0
99.5
99.0
98.5
98.0
97.5
97.0
96.5
96.0
Weight (%)
-0.69%
-1.66%
-1.15%
0.020
0.015
0.010
0.005
0.000
-0.005
-0.010
-0.015
-0.020
-0.025
Derivative weight (%/°C)
0.30
0.25
0.20
0.15
0.10
0.05
0.00
-0.05
-0.10
-0.15
Heat flow (W/g)
100
200
300
400
500
Temperature (°C)

c)

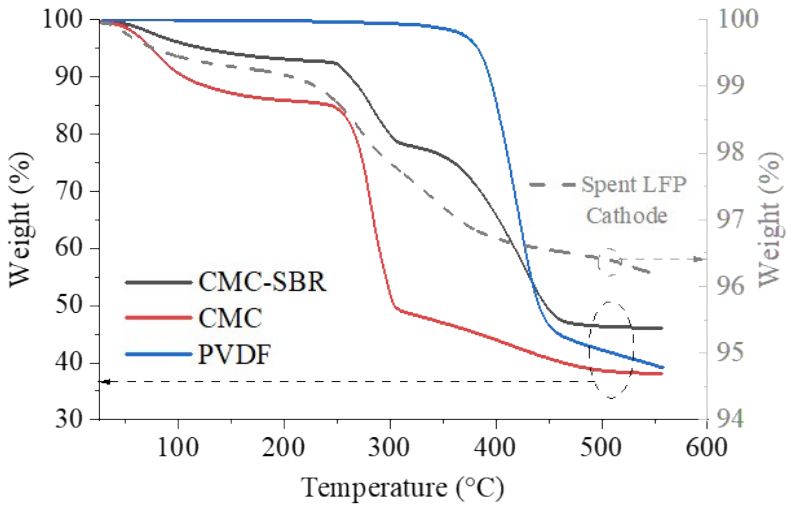

d)

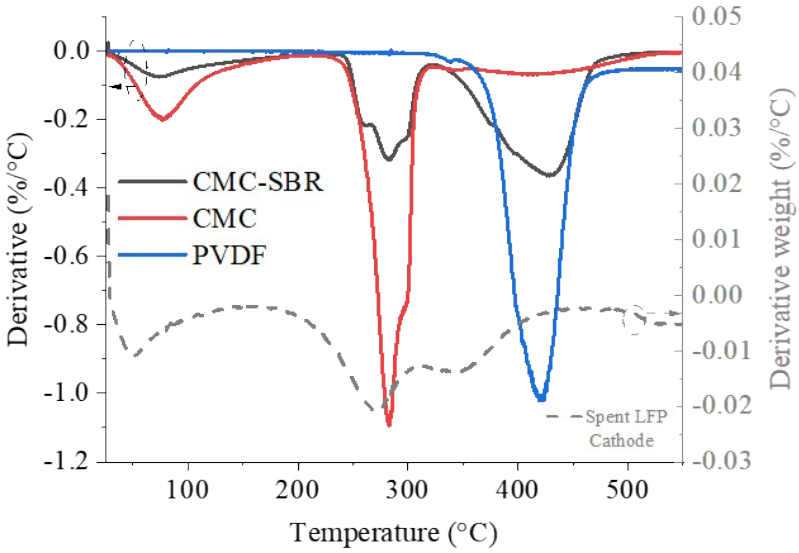

Figure S2: Thermal analysis of: a) Comparison of TGA curves of spent $LiFePO_4$ cathode sample (black), mixed commercial $LiFePO_4$ with carbon black and CMC-SBR at a weight ratio of 90:5:5 in water and coated on aluminium foil (red), and mixed commercial $LiFePO_4$ with carbon black and PVDF at a weight ratio of 90:5:5 in NMP and coated on aluminium foil (blue), while b) spent $LiFePO_4$ cathode, including TGA (black), DTG (red), and DSC (blue) graphs, and c) and d) are the TGA and DTG curves, respectively, of CMC-SBR mixture, pure CMC, and PVDF binders

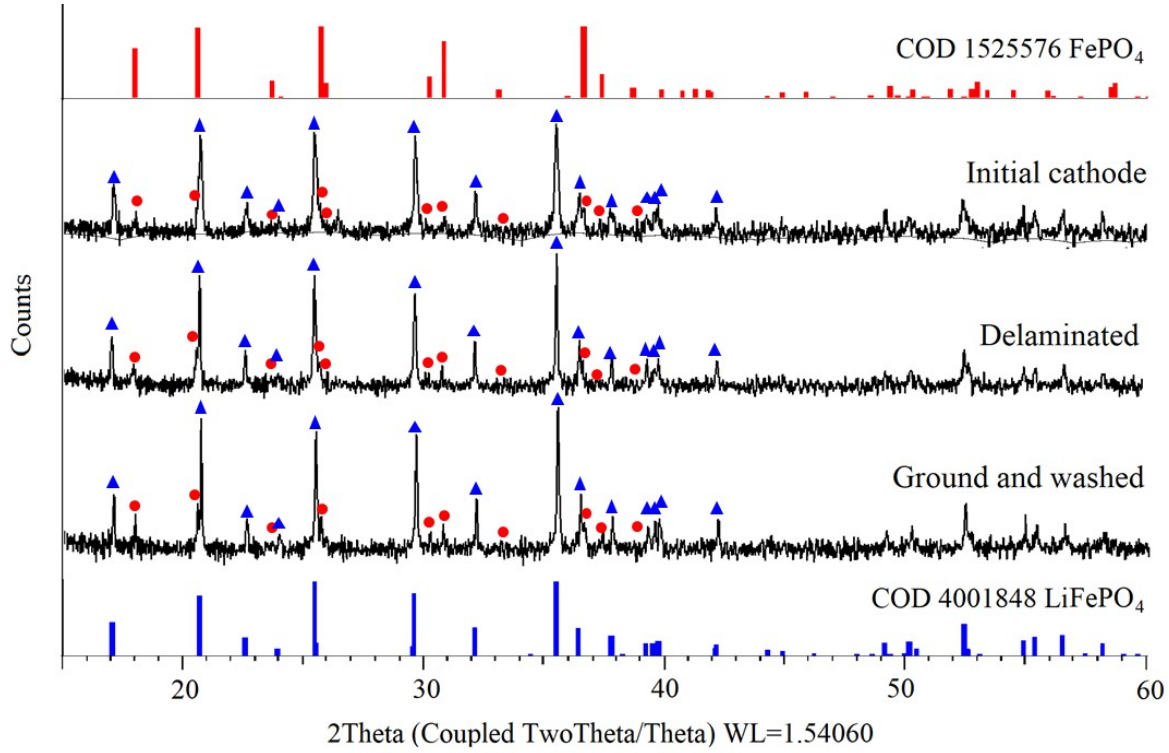

Figure S3: XRD patterns of the initial cathode, dried delaminated, and ground materials.

Screening of organic reducing agents

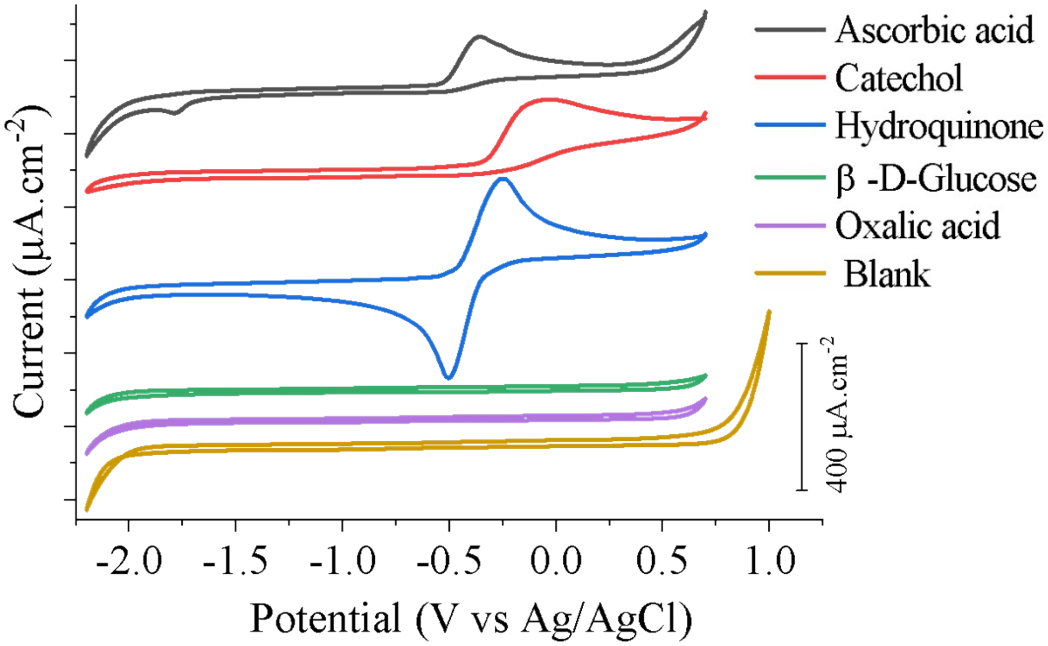

Figure S4: Cyclic voltammograms of 20 mmol dm^{-3} of different catalysts in $LiOAc{\cdot}2H_2O$: 3EG solution. Scans are recorded at 25 °C at a scan rate of 20 mV s^{-1}, using a graphite disk working electrode, and an aqueous 3.0 mol dm^{-3} KCl silver/silver chloride reference electrode.

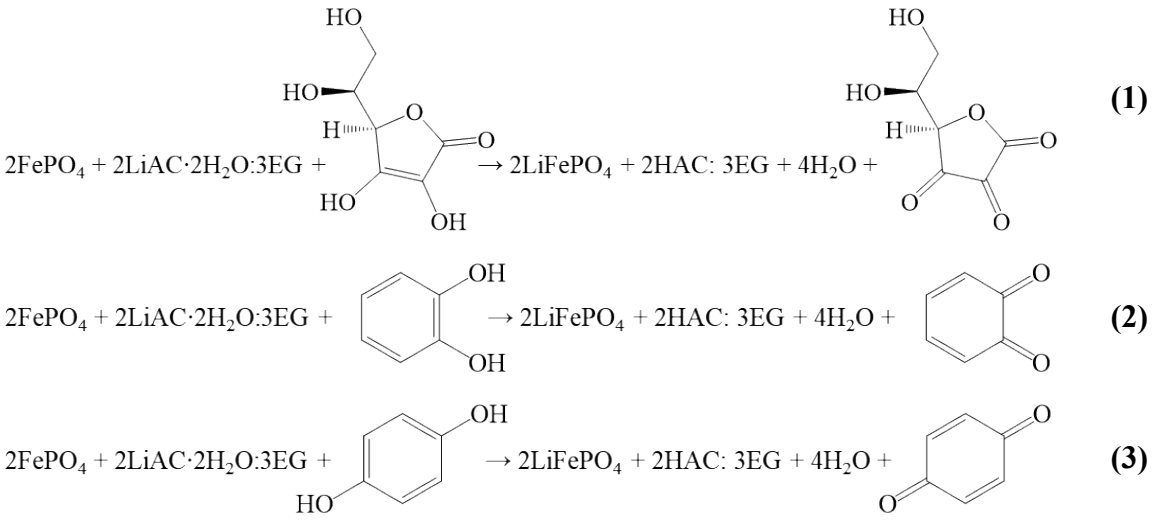

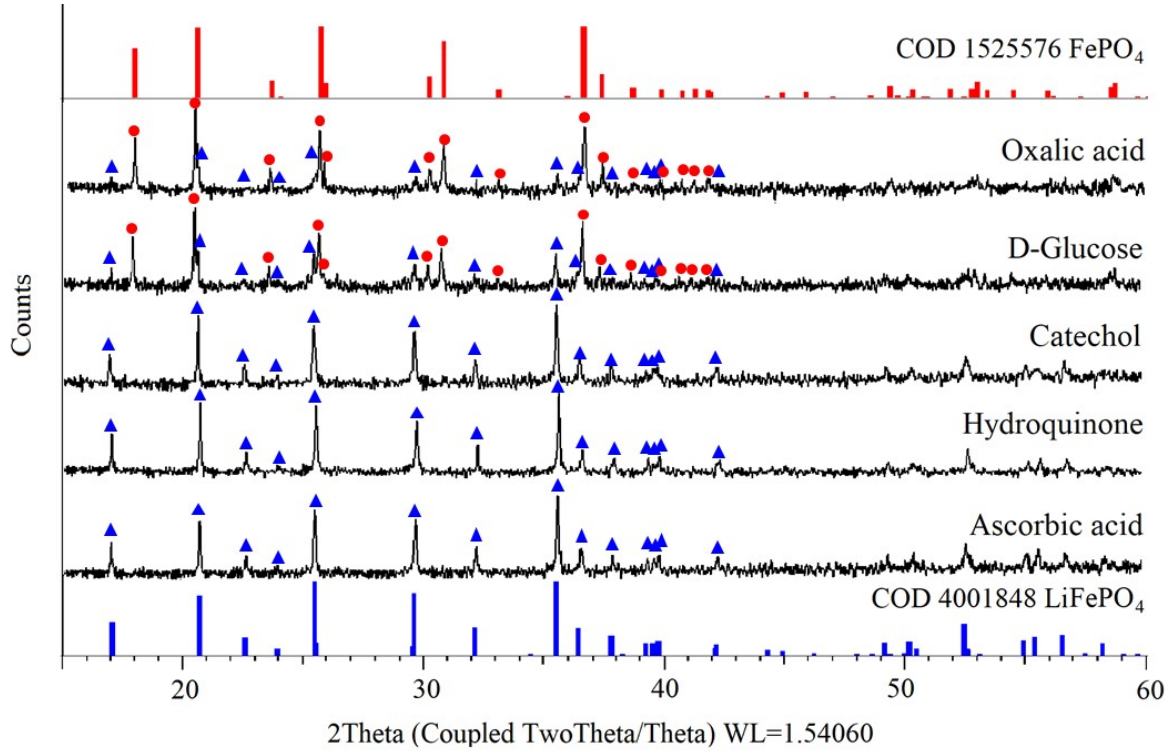

Figure S5: XRD patterns of the re-lithiated material using different organic oxidising agents in $LiOAc{\cdot}2H_2O$: 3EG solution at 50 °C for 5 h, included are reference patterns for $FePO_4$ and $LiFePO_4$ (initial material was the $FePO_4$ powder obtained after oxidative leaching).

Direct reductive re-lithiation

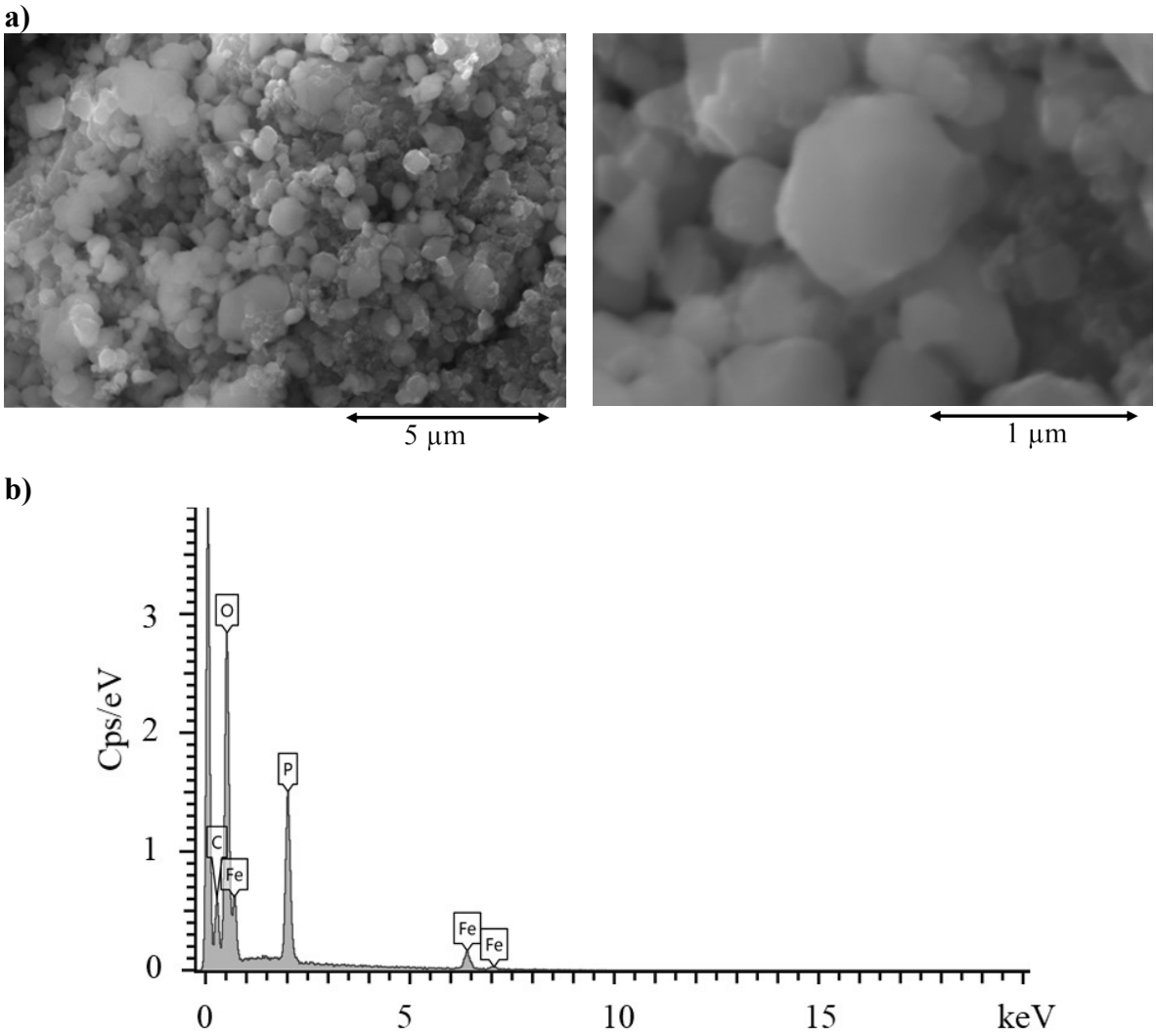

Figure S6: SEM images (a and b), EDX spectra (c) directly reductive regenerated $LiFePO_4$ with 1.74 mol dm^{-3} hydroquinone in $LiOAc{\cdot}2H_2O$: 3EG at 25 °C for 1 hr

Table S3 EDX elemental composition of directly reductive regenerated $LiFePO_4$ with 1.74 mol dm^{-3} hydroquinone in $LiOAc{\cdot}2H_2O$: 3EG at 25 °C for 1 hr

Element	Wt%	Atomic%	Atomic ratio
C	14.88(1.99)	26.31(3.72)	2.37(0.61)
O	38.56(7.46)	50.80(7.13)	4.71(1.68)
P	16.45(1.60)	11.33(1.81)	1.00(0.11)
Fe	30.00(6.03)	11.51(3.08)	1.00(0.00)

Atomic ratio is calculated refer to Fe.

Oxidative leaching and reductive re-lithiation

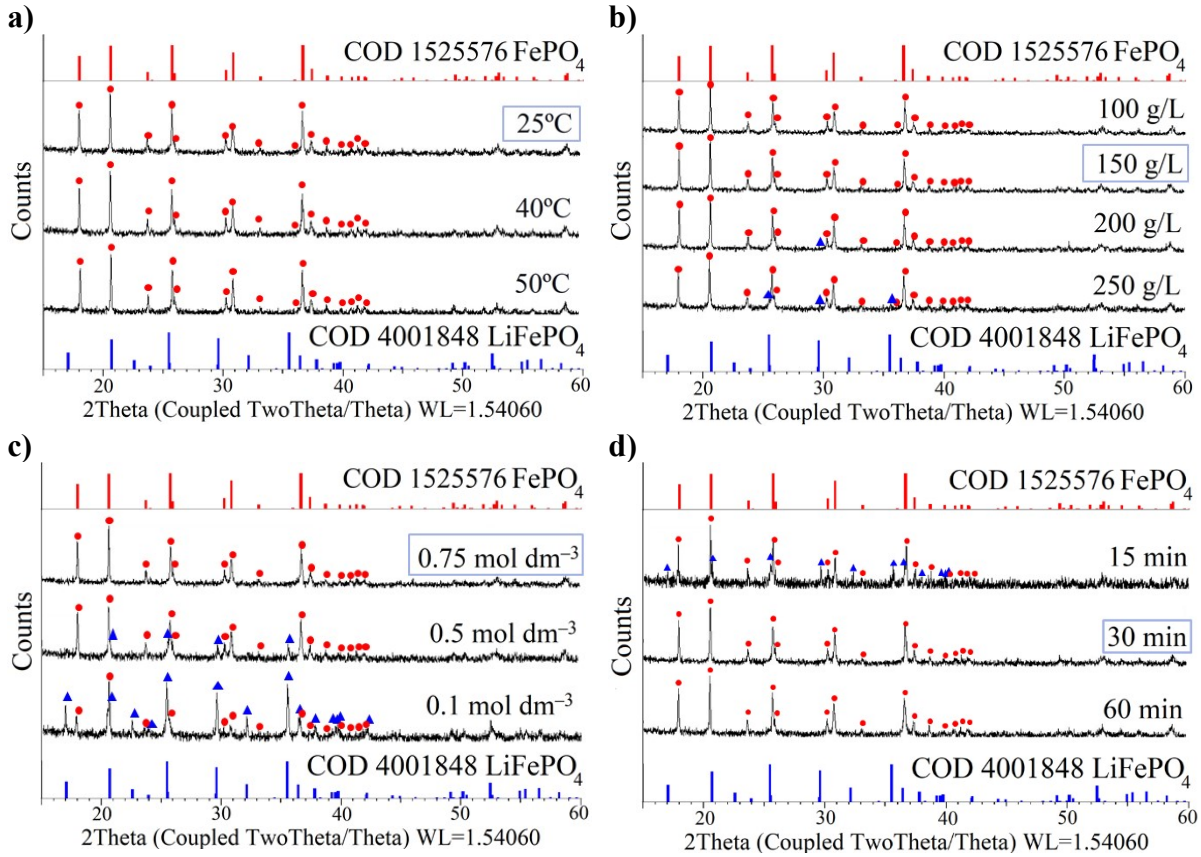

Figure S7: The effects of (a) temperature (under the conditions of 1 mol dm^{-3} $FeCl_3$ in water for 3 h 50 g L^{-1}), (b) S/L ratio (under the conditions of 1 mol dm^{-3} $FeCl_3$ in water for 3 h 25 °C), (c) concentration of $FeCl_3$ in water (under the conditions of 3 h, 150 g L^{-1} and 25 °C), and (d) time (under the conditions of 0.75 mol dm^{-3} in water and 150 g L^{-1} 25 °C) on XRD patterns of oxidative leaching process.

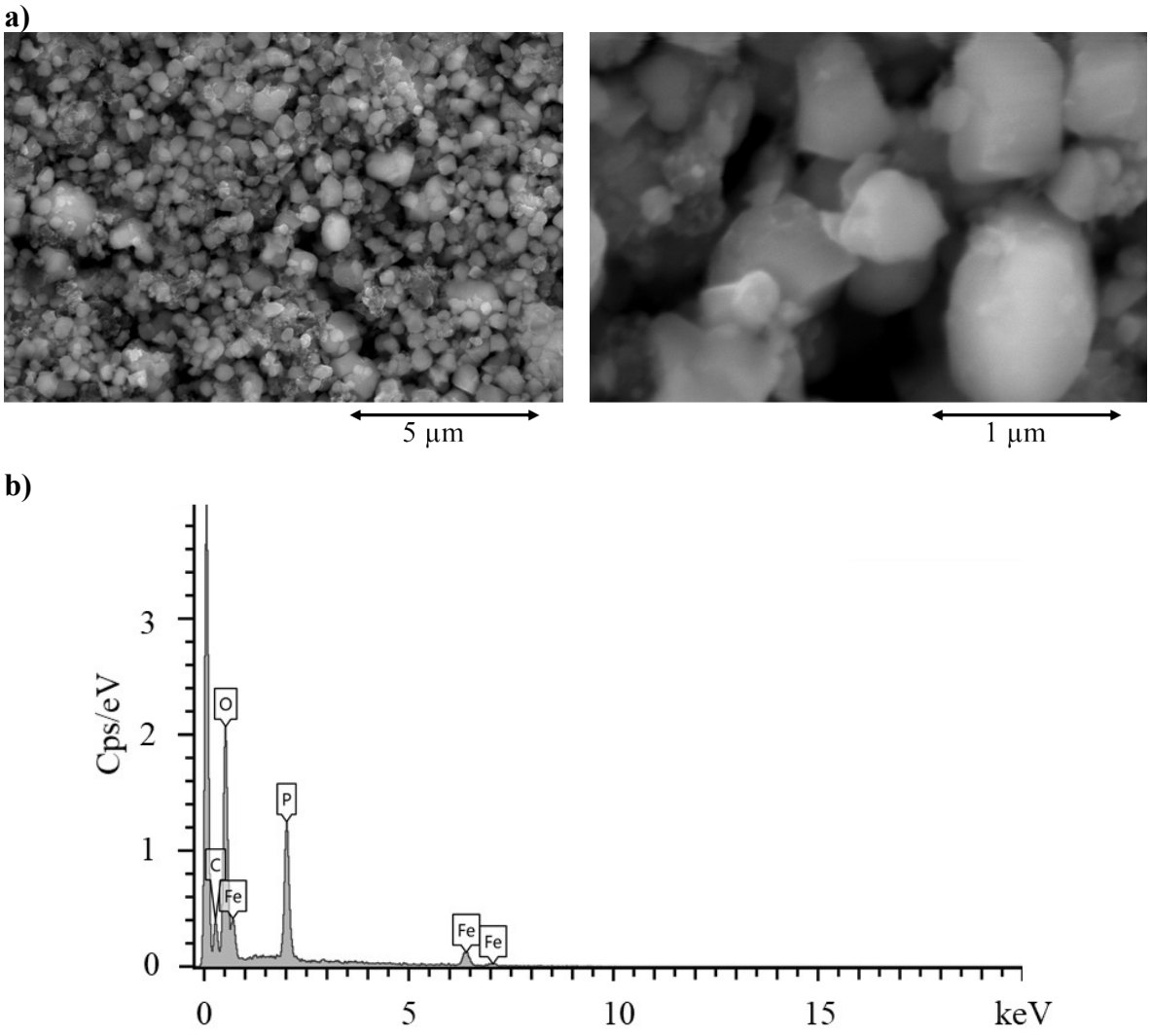

Figure S8: SEM images (a and b), EDX spectra (c) of oxidative leached, followed by reductive regenerated $LiFePO_4$ with 1.74 mol dm^{-3} hydroquinone in $LiOAc{\cdot}2H_2O$: 3EG at 25 °C for 3 h.

Table S4 EDX elemental composition of oxidative leached, followed by reductive regenerated $LiFePO_4$ with 1.74 mol dm^{-3} hydroquinone in $LiOAc{\cdot}2H_2O$: 3EG at 25 °C for 3 h.

Element	Wt%	Atomic%	Atomic ratio
C	16.03(1.67)	26.69(1.64)	3.03(0.78)
O	43.46(5.42)	54.25(3.86)	6.20(1.72)
P	15.18(1.94)	9.88(1.90)	1.09(0.06)
Fe	25.34(4.73)	9.17(2.31)	1.00(0.00)

Atomic ratio is calculated refer to Fe**.**

Table S5 Detected elements in solutions (ppm) after oxidative leaching and reductive regenerated $LiFePO_4$ from $FePO_4$, analysed by ICP-MS

Element	Leached solution (ppm)	Re-lithiated solution (ppm)
Li	3941.79	N/A
P	287.25	355.46
Fe	N/A	1223.03

Table S6 atomic percentage of spent LFP, powder after direct re-lithiation, powder after oxidative leaching and re-lithiated of leached powder (results calculated from ICP-MS).

Element	Spent LFP (atomic %)	Direct re-lithiated (atomic %)	Leached powder (atomic %)	Re-lithiated leached powder (atomic %)
7Li	0.91	1.00	0.02	0.61
57Fe	1.00	1.00	1.00	1.00
31P	0.99	1.02	0.97	1.01

57Fe is selected from Collision Mode (Kinetic Energy Discrimination, KED). Mole ratio is calculated refer to Fe. The isotopes are selected from gives the closest match (R-squared, R^2 closest to 1) to of the calibration curves.

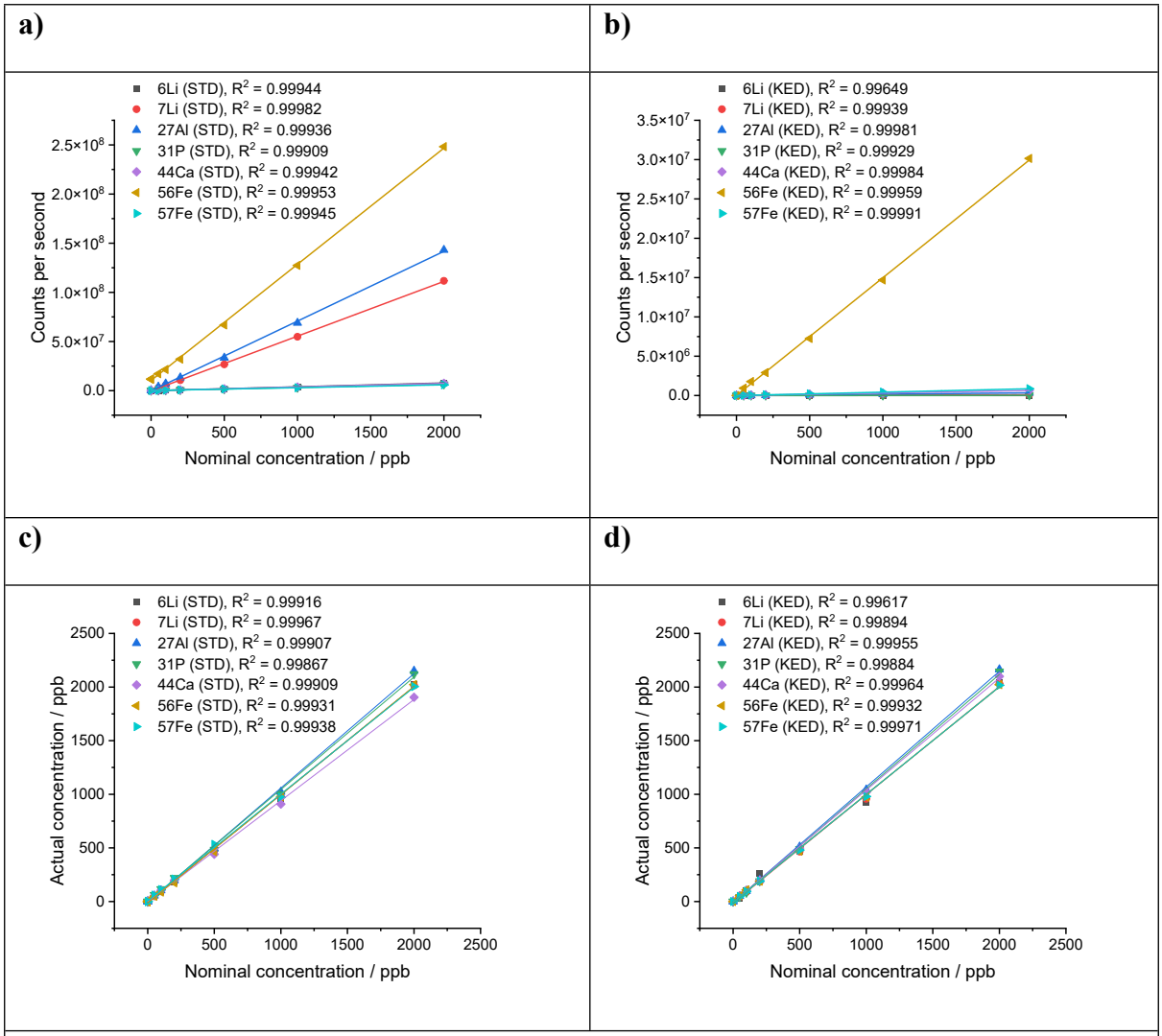

Figure S9: Calibration curves for the ICP-MS calibration solutions. a) STD in counts per second, b) KED in counts per second, c) STD in ppb, and d) KED in ppb.

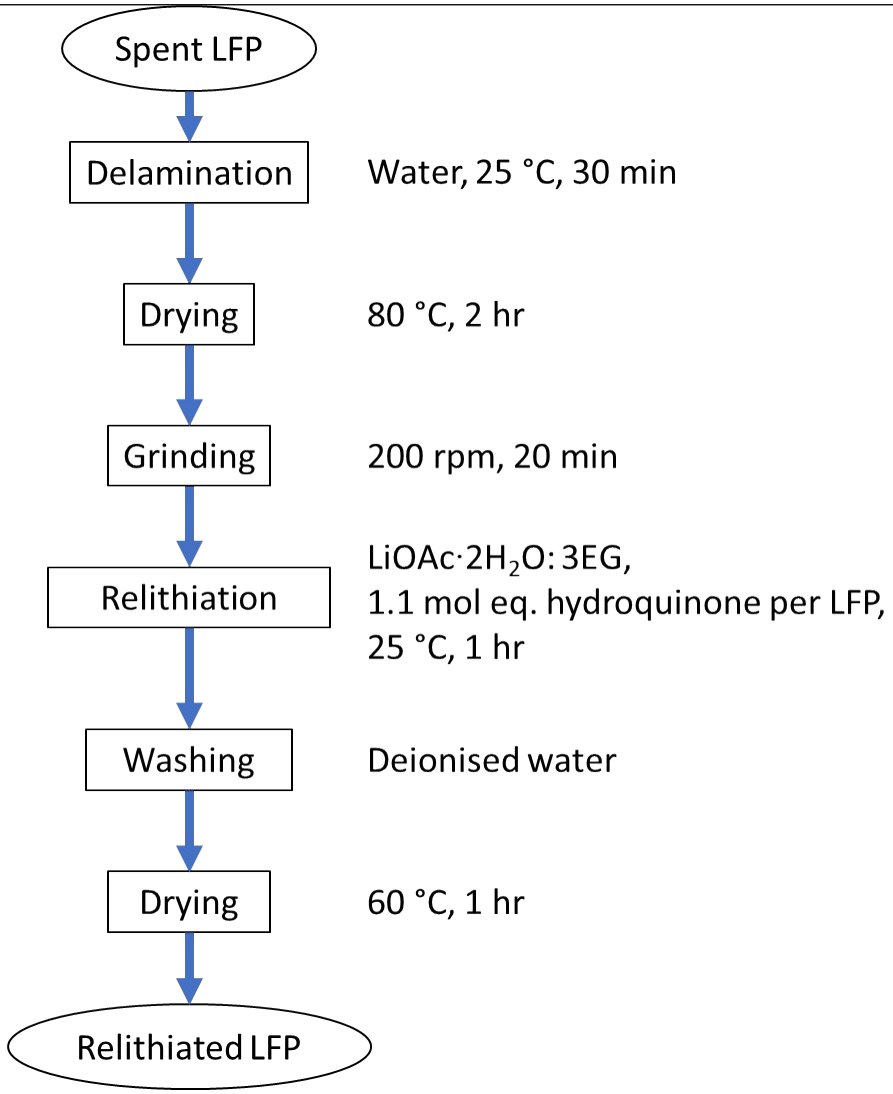

Figure S10: Detailed flowsheet of the direct regeneration process presented in Figure 1c.

References

1. R. P. Santoro and R. E. Newnham, *Acta Crystallographica*, 1967, **22**, 344-347.
2. A. K. Padhi, K. S. Nanjundaswamy and J. B. Goodenough, *Journal of The Electrochemical Society*, 1997, **144**, 1188-1194.
3. J. Li and Z.-F. Ma, *Chem*, 2019, **5**, 3-6.
4. A. Yamada, S. C. Chung and K. Hinokuma, *Journal of The Electrochemical Society*, 2001, **148**, A224.
5. S.-Y. Chung, J. T. Bloking and Y.-M. Chiang, *Nature Materials*, 2002, **1**, 123-128.
6. X.-Z. Liao, Z.-F. Ma, L. Wang, X.-M. Zhang, Y. Jiang and Y.-S. He, *Electrochemical and Solid-State Letters*, 2004, **7**.
7. D. L. Thompson, J. M. Hartley, S. M. Lambert, M. Shiref, G. D. J. Harper, E. Kendrick, P. Anderson, K. S. Ryder, L. Gaines and A. P. Abbott, *Green Chemistry*, 2020, **22**, 7585-7603.

8. F. Forte, M. Pietrantonio, S. Pucciarmati, M. Puzone and D. Fontana, *Critical Reviews in Environmental Science and Technology*, 2021, **51**, 2232-2259.
9. D. Latini, M. Vaccari, M. Lagnoni, M. Orefice, F. Mathieux, J. Huisman, L. Tognotti and A. Bertei, *Journal of Power Sources*, 2022, **546**, 231979.
10. J. Ha, S.-K. Park, S.-H. Yu, A. Jin, B. Jang, S. Bong, I. Kim, Y.-E. Sung and Y. Piao, *Nanoscale*, 2013, **5**, 8647-8655.
11. F. Pignanelli, M. Romero, D. Mombrú, E. Téliz, V. Díaz, J. Castiglioni, F. Zinola, R. Faccio and Á. W. Mombrú, *Ionics*, 2019, **25**, 3593-3601.
12. Q. Li, Z. Zhou, S. Liu and X. Zhang, *Ionics*, 2016, **22**, 1027-1034.